Iranian Society of Acoustics and Vibration
The 14th ISAV2024 International Conference on Acoustics and Vibration
11-12 Dec 2024 Karaj - Iran
Kharazmi University

CFD ANALYSIS OF VORTEX SHEDDING AND FREQUENCY CHARACTERISTICS OF A NACA 63-415 AIRFOIL AT HIGH REYNOLDS NUMBERS

Hooman Mirzaee[a], Mostafa Esmaeili[b*]

[a] *Bachelor of Science, Department of Mechanical Engineering, Kharazmi University, 15719-14911, Tehran, Iran.*

[b] *Accosiate Professor, Department of Mechanical Engineering, Kharazmi University, 15719-14911, Tehran, Iran.*

* *Corresponding author e-mail: m.esmaeili@khu.ac.ir*

Abstract

In order to preclude vibration and resonance, the vortex shedding characteristics have been numerically simulated at Re = 1.042 × 10^6 using computational fluid dynamics (CFD), focusing on flow separation from the NACA 63-415 airfoil. In addition, the variation of vortex shedding forms and the corresponding frequency characteristics at various angles of attack are studied. The 2-D simulation consists of two stages: steady analysis and transient analysis, with ANSYS fluent utilized for this research. The purpose of steady-state approach is to comprehensively validate the model's results by comparing them with available experimental data, as well as to study grid independence. The Spalarat-Allmaras model is used for simulating the airfoil in the steady-state, while the k-ω SST model is used for the unsteady part. The frequency spectrum corresponding to the lift coefficient is used to analyze the of vortex shedding characteristics from a frequency domain perspective. In other words, Power spectral densities of the unsteady lift and drag coefficients are used to determine flow characteristics. By increasing the angle of attack, the Strouhal number of vortex shedding frequency increases, and the stability of the flow field decreases. Large and damaging vibrations can occur if the vortex shedding frequency becomes close to the natural frequency of the structure.

Keywords: Vortex shedding; Lift and drag coefficients; Flow separation; Strouhal number.

1. Introduction

The fluid dynamics around airfoils is one of the most significant problems in fluid mechanics, which has long been of interest, and many studies have been conducted to enhance the comprehension of flow separation and vortex shedding phenomena. This phenomenon, which first investigated in the laboratory by Strouhal [1], has a significant impact on increasing the drag coefficient, root mean square of the lift coefficient, and structural vibrations. On some occasions, however, the shedding leads to a reduction in drag, which is a desirable feature in many applications [2]. Theodore von Kármán linked this phenomenon to the stable, staggered vortices that form behind a cylindrical object, later termed the Kármán vortex street effect. In addition, he proposed the theory of vortex street stability [3]. Vibrations caused by vortex shedding are a well-known phenomenon in structure-fluid interaction and occur when a structure oscillates in various engineering applications, such as offshore risers, oil pipelines, bridges, chimneys, tall buildings, and electric cables. When the vortex shedding frequency is close to the natural frequency of the structure, the vibrations become more intense, leading to the phenomenon of resonance, which may cause structural fatigue and even instability. Given that vibration caused by vortex is one of the most important factors of fatigue and structural instability, investigating ways to reduce or suppress these vibrations has drawn the attention of many researchers. Methods to control vortex-induced vibration include changing the object's geometry and orientation, as well as utilizing optimization techniques to find the best shape for a given circumstance. For instance, varying the airfoil's angle of attack alters the stability of the flow field. Additionally, the presence of sharp edges on a bluff body is important in improving the accuracy and consistency of the vortex shedding phenomenon [4].

Airfoil aerodynamics in the stall and post-stall regimes indicate sophisticated aspects strongly dependent on the Reynolds number and angle of attack. Many previous investigations have studied the wake characteristics of flow over airfoils at low Reynolds numbers and low angles of attack, but research on stall and post-stall conditions (higher angles of attack) at high Reynolds numbers is less extensive. Zhou et al. [5] provided information about the mean and fluctuating forces on a NACA-0012 airfoil at Re = 5,000 and 50,000 over a wide range of angles of attack up to 90 degrees. The present study is compared to the information provided by Bak et al. [6]. Alam et al. [7] conducted experiments on the flow structure in the wake of a NACA-0012 airfoil under the same conditions as Zhou et al. [5]. They presented wake and force measurements and discussed vortex formation, shedding, and variations in its frequency and size with the angle of attack. In a study on a NACA-0012 airfoil, Chang et al. [8] investigated the characteristics of vortex shedding frequency and its relationship with different angles of attack at low Reynolds numbers. Chang et al. [8] numerically simulated the flow field at various angles of attack and analyzed the relationship between the vortex shedding frequency around the trailing edge and the variation trend of the airfoil's lift and drag coefficients. Consequently, the results showed that the flow field gradually transitions from steady to unsteady state, and for $\alpha>7$, conspicuous vortex shedding manifests. the stability and Strouhal number decrease with increasing the angle of attack. Additionally, according to Ramesh et al. [9], increasing the leading edge radius of an SD7003 airfoil caused the critical leading edge suction power (LESP) to rise, meaning that a more rounded leading edge can better handle suction and reduce the probability of flow separation. Achenbach and Heinecke [10] conducted wind tunnel experiments and discovered that the wake of a cylinder became more regular as the cylinder’s surface roughness increased. Furthermore, the Strouhal number of a vortex shedding from a rough cylinder was estimated to be much smaller than that from a smooth cylinder.

According to the aforementioned experiments, it is evident that angle of attack and geometry play crucial roles in this concept. In this paper, a numerical simulation of the flow field at various angles of attack is conducted, and the relationship between vortex shedding frequency and angle of attack is explored. Due to the lack of adequate experimental data for the unsteady section of this specific airfoil, a steady-state study is first conducted to validate the results by comparing the lift and drag coefficients comparison with the real data from Bak et al. [6], as well as checking the pressure coefficient graph. After ensuring the reliability of the utilized model in ANSYS Fluent, an unsteady simulation is conducted using the same model to calculate the vortex shedding frequency. For this purpose, extracted power spectral density and fluctuating graphs of the lift and drag coefficients are analyzed. Additionally, the Strouhal number and its variation corresponding to the generated frequency are explored for further understanding.

2. Physical model and numerical methods

2.1 Boundary conditions, grid and domain of calculation

The boundary conditions and calculation domain related to the flow around the NACA 63-415 are shown in Fig. 1, along with the grid structure in Fig. 2. The chord of the airfoil is c = 0.507 m. The Reynolds number is Re = 1.042 × 10^6 (u_0 = 30 m/s). As shown in Fig. 1, the left boundary condition is velocity inlet, and pressure outlet is adopted for the right boundary condition. A symmetry condition is utilized for the top and bottom horizontal boundaries, as no stress is present. A no-slip wall boundary condition is applied the surface of the airfoil.

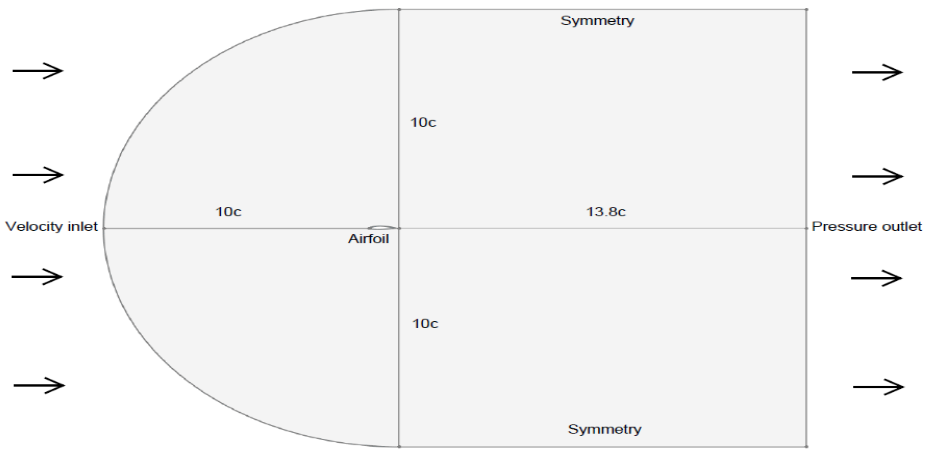

Figure 1. Boundary conditions and calculation domain of NACA 63-415.

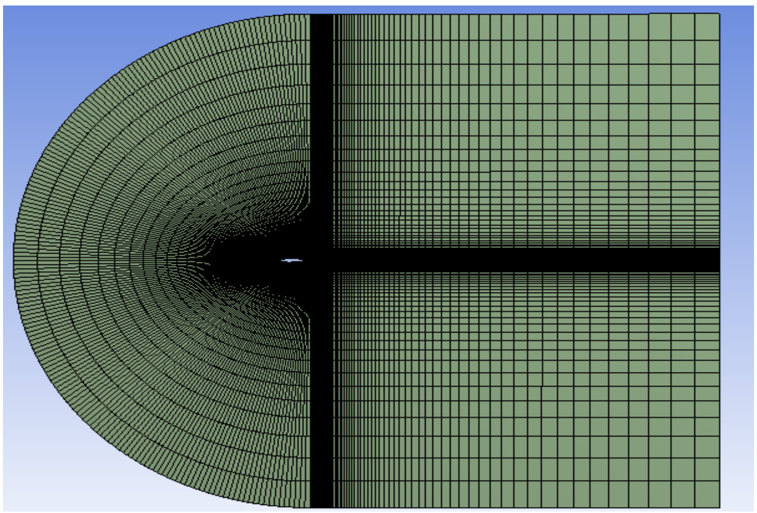

(a) Gobal grid

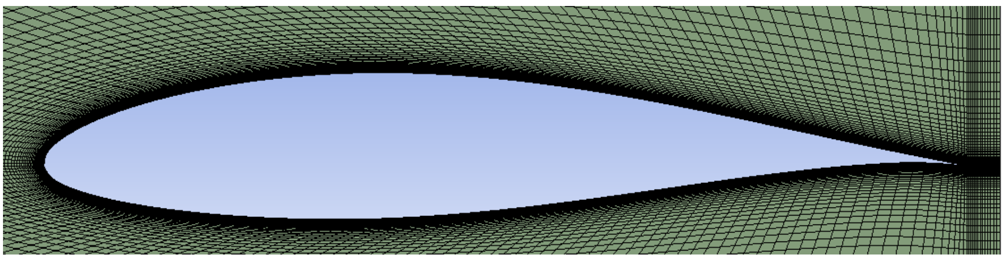

(b) Grid near airfoil

Figure 2. Grid structure diagram of NACA 63-415.

2.2 Numerical methods and equations

Since the simulation is two-dimesional and the flow is incompressible, the governing equations, which are the continuity equation and Navier-Stokes equations, can be expanded into a simplified form.

The continuity equation for this flow field is

$$\frac{\partial u}{\partial x} + \frac{\partial v}{\partial y} = 0 \tag{1}$$

The Navier-Stokes equations for this flow field are

$$\rho\left(\frac{\partial u}{\partial t} + u\frac{\partial u}{\partial x} + v\frac{\partial v}{\partial y}\right) = -\frac{\partial p}{\partial x} + \rho g_x \ + \mu\left(\frac{\partial^2 u}{\partial x^2} + \frac{\partial^2 u}{\partial y^2}\right) \tag{2}$$

$$\rho\left(\frac{\partial v}{\partial t} + u\frac{\partial v}{\partial x} + v\frac{\partial v}{\partial y}\right) = -\frac{\partial p}{\partial y} + \rho g_y \ + \mu\left(\frac{\partial^2 v}{\partial x^2} + \frac{\partial^2 v}{\partial y^2}\right) \tag{3}$$

In these equations, v is the velocity in the y-direction and u is the velocity in the x-direction. t is the time, p is the pressure, ρ is the mass density, μ is the viscosity, g_x and g_y are gravitational accelerations in x- direction and y-direction, respectively.

The Spalart-Allmaras model is used for the steady analysis. The shear-stress transport (SST) k-ω model is utilized for the transient analysis.

2.3 Model accuracy verification

To validate the utilized model, the results of the steady analysis are compared to the data from Bak et al. [6]. Since Spalart-Allmaras model is used for this section, the Y^+ parameter should be kept small for better accuracy. Thus, the criterion $Y^+ \leq 1$ should be met.

The lift and drag coefficient graphs for the steady state are determined for various angles of attack in the range of 0^o~15^o at Re =.1.042 × 10^6. As shown in Fig. 3, the calculated lift and drag coefficients fit reasonably with the results of Bak et al. [6]. The curves in Fig. 3 reflect the variation law of airfoil lift and drag coefficients, and the maximum error remains within 10%.

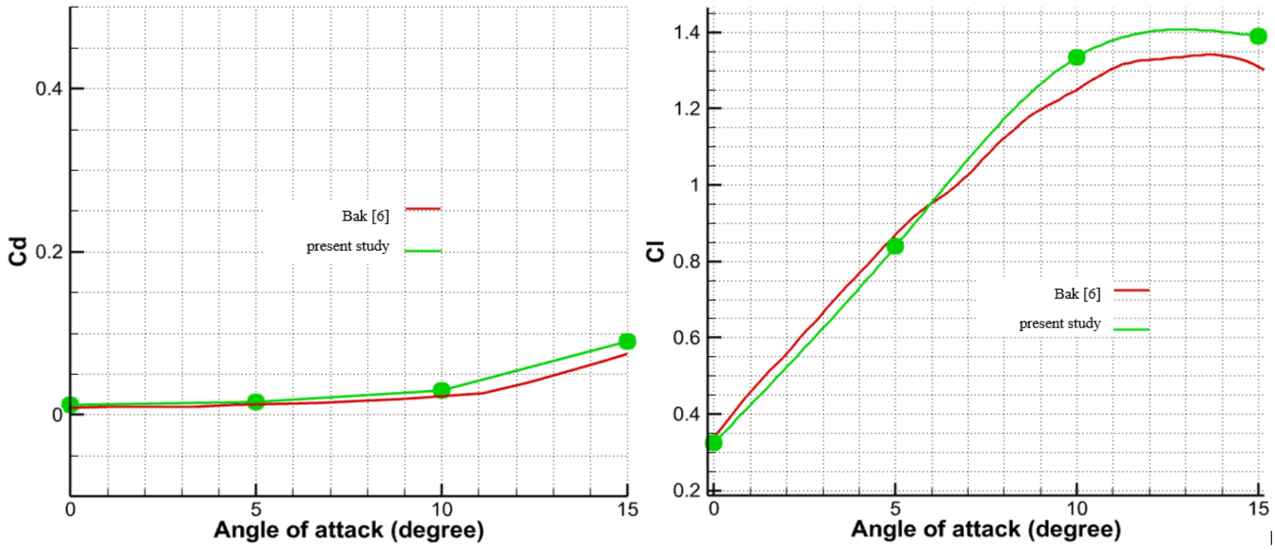

Figure 3. Drag and lift coefficients values in various angles of attack.

3. Results and discussion

After conducting the steady simulation to verify the model's accuracy, an unsteady simulation is performed at Re =.1.042 × 10^6 utilizing the shear-stress transport (SST) k-ω model at various angles of attack. At low angles of attack, there is insufficient flow separation for vortex shedding to occur. However, at α = 25°, vortex shedding begins. The time step used in these simulations is Δt = 0.005 s.

Table 1. Lift and drag coefficient graphs over a duration of 0.5 s.

Angle of attack	Lift coefficient graph	Drag coefficient graph
15°	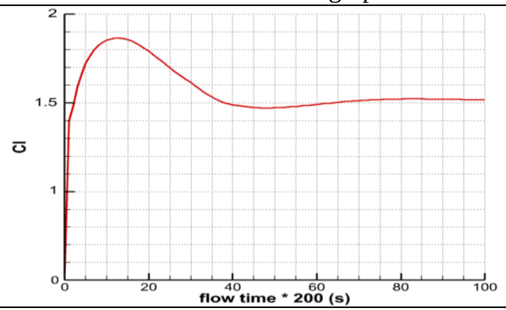	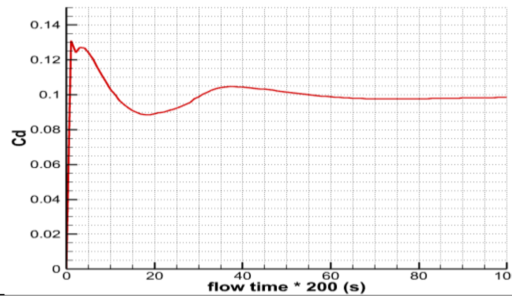
25°	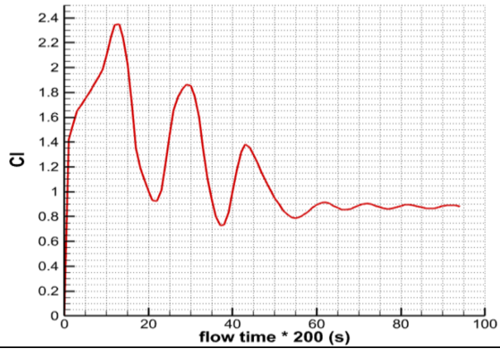	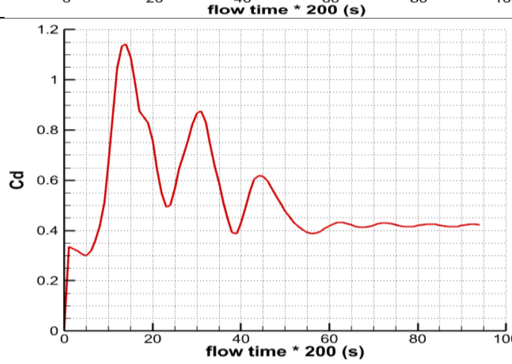

35º	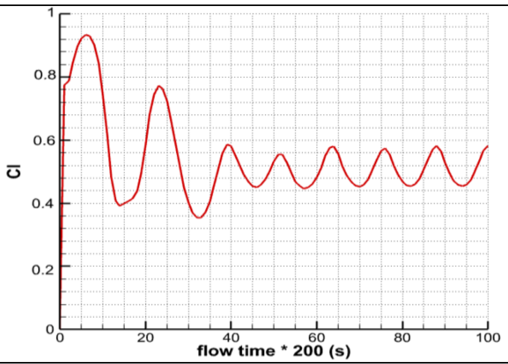	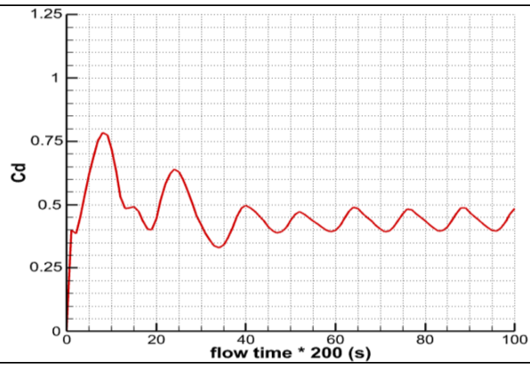
50º	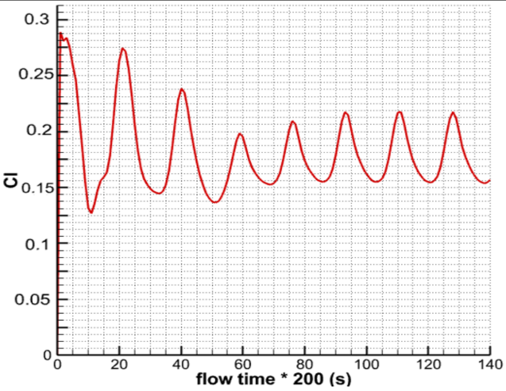	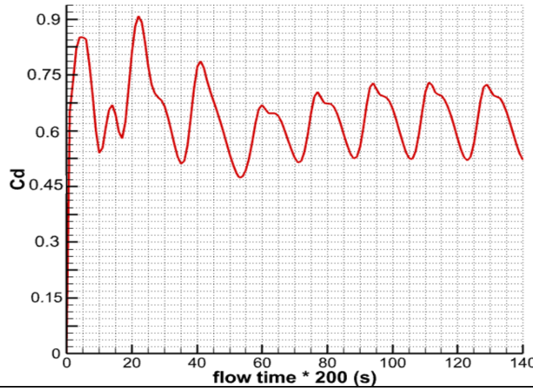

As shown in Table 1, the values of the lift and drag coefficients fluctuate around the calculated steady values at the corresponding angles of attack after a period of time. Although the stall phenomenon should occur at α ≈ 13º, the separation is not sufficient for the creation of vortex shedding. Therefore, at higher angles of attack (α = 25º), this phenomenon commences happening. To calculate the frequency of the available vortex shedding, power spectral density is determined using the lift coefficient data at each angle of attack.

Table 2. Airfoil's velocity contour at various angles of attack.

AOA	Velocity contour
25º	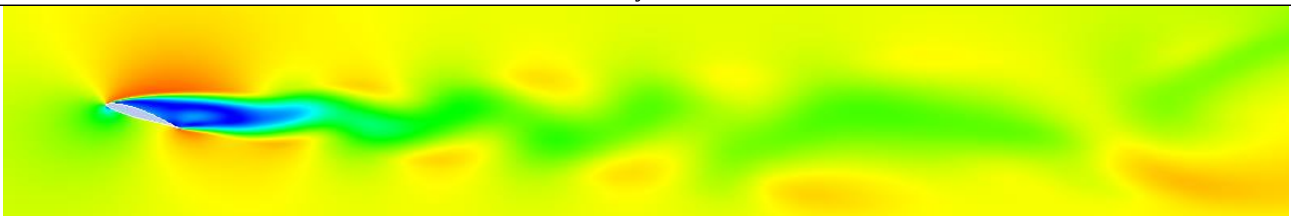
35º	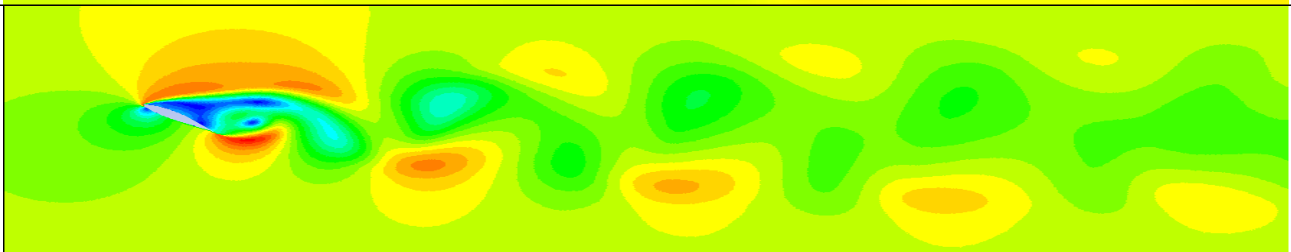
50º	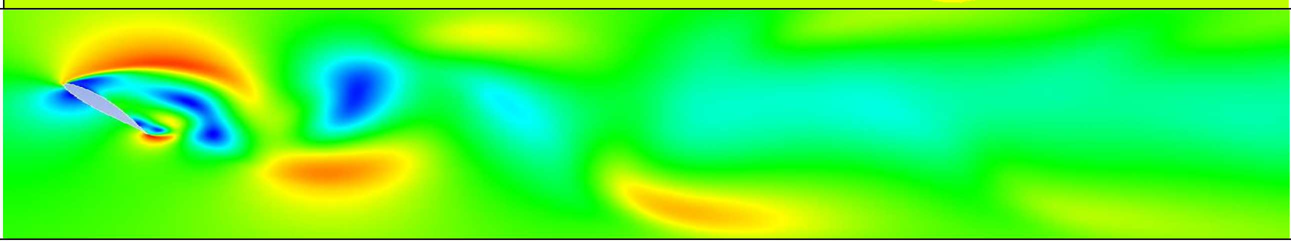

Table 3. Airfoil's pressure contour at various angles of attack.

AOA	Pressure contour
25º	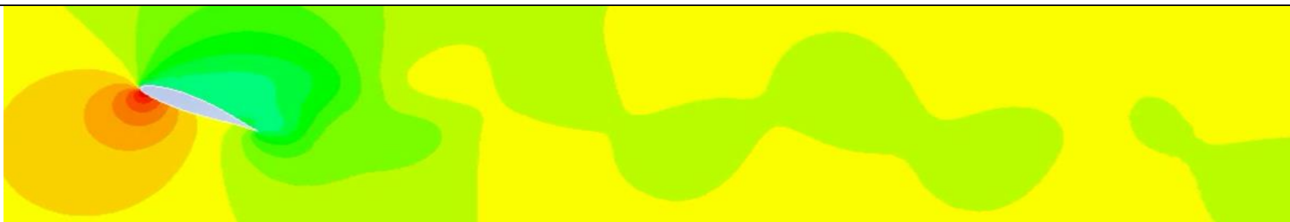
35º	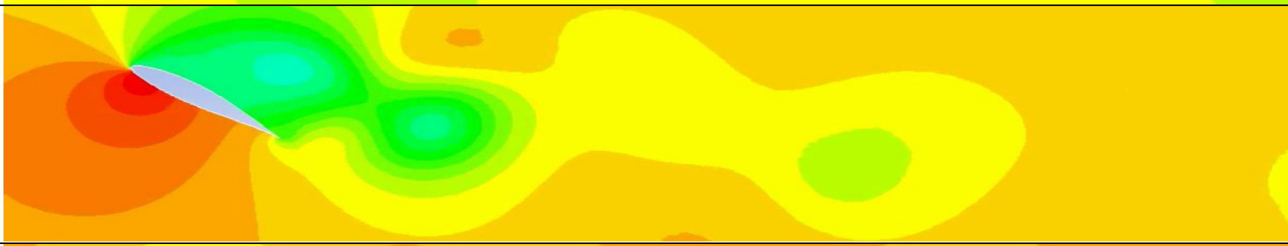
50º	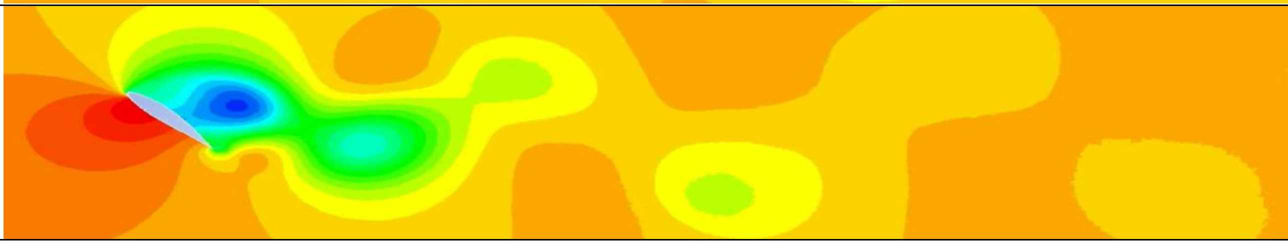

Table 4. Determined Power spectral density graphs at various angles of attack.

Angle of attack	Power spectral density graph	Vortex shedding frequency	Strouhal number
25º	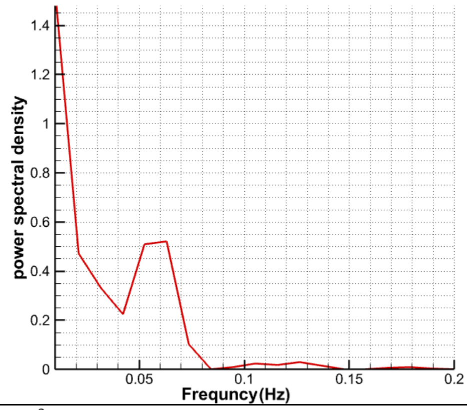	0.06315 Hz	0.00045
35º	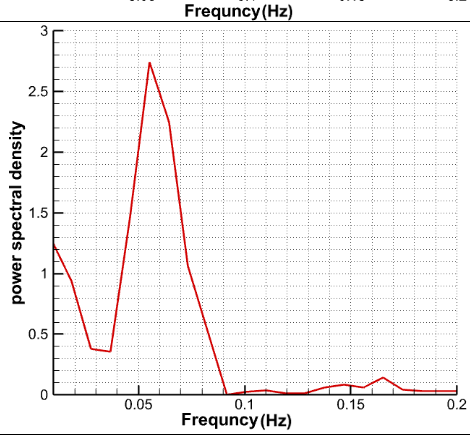	0.05504 Hz	0.00053

50º	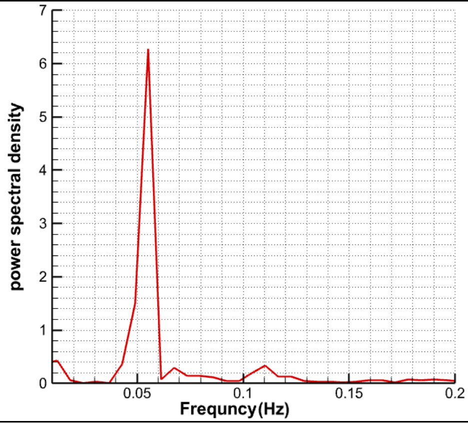	0.05421 Hz	0.00075

As shown in table 4, as the angle of attack increases, the Strouhal number exhibits an upward trend, demonstrating a rise in the amplitude of fluctuations in the lift and drag coefficient graphs, whereas the frequency of vortex shedding decreases.

4. Conclusion

In this paper, the trend of flow instability variations and vortex shedding characteristics with raising the angle of attack of the NACA 63-415 airfoil at Re = 1.042×10^6 has been studied. As the angle of attack increases, the stability of the flow decreases, and the amplitude of in the lift and drag coefficient graphs increases. Although the airfoil reaches stall at $\alpha \approx 13^o$, flow separations are barely visible and insufficient for vortex shedding to form. The first noticeable vortex shedding occurs at $\alpha = 25^o$. As the angle of attack increases, the intensity of flow separation rises, vortex shedding frequency decreases, and the Strouhal number experiences an upward trend. From the extracted data, It can be interpreted that a higher Strouhal number corresponds to an increase in the amplitude of fluctuations in the lift and drag coefficient graphs.

REFERENCES

1. V. Strouhal, *Über eine besondere Art der Tonerregung*, Stahel, 1878.
2. S. Tang, A. Aubry, "Suppression of vortex shedding inspired by a low-dimensional model", *Journal of Fluids and Struct*ures 14, No. 4, 443-468 (2000).
3. L.M. Milne-Thomson, *Theoretical Hydrodynamics*, Macmillan, London, UK, 1972; p. 375.
4. S. Mittal, A. Raghuvanshi, "Control of vortex shedding behind circular cylinder for flows at low Reynolds numbers", *International Journal For Numerical Methods In Fluids* 35, 421-447 (2001).
5. Y. Zhou, M.M. Alam, H. Yang, H. Guo and D. Wood, "Fluid forces on a very low-Reynolds-number airfoil and their prediction", *International Journal of Heat and Fluid Flow* 32, No. 1, 329–339 (2011).
6. C. Bak, P. Fuglsang, J. Johansen and I. Antoniou, "Wind Tunnel Test of NACA 63-415 and a Modified NACA 63-415 Airfoil", *Forskningscenter Risoe.* Risoe-R No. 1193(EN), Denmark (2000).
7. M.M. Alam, Y. Zhou, H. Yang, H. Guo and J. Mi, "The ultra-low Reynolds number airfoil wake", *Experiments in Fluids* 48, No. 1, 81–103 (2010).
8. J. Chang, Q. Zhang, L. He and Y. Zhou, "Shedding vortex characteristics analysis of NACA 0012 airfoil at low Reynolds numbers", *International Conference on New Energy and Power Engineering (ICNEPE 2021)*, Sanya, China, November 19-21 (2021).

9. K. Ramesh, J. Ke, A. Gopalarathnam and J. R. Edwards, "Effect of Airfoil Shape and Reynolds Number on Leading Edge Vortex Shedding in Unsteady Flows", *30th AIAA Applied Aerodynamics Conference,* New Orleans, Louisiana, June 25-28 (2012).

10. E. Achenbach, E. Heinecke, "On vortex shedding from smooth and rough cylinders in the range of Reynolds numbers 6×10^3 to 5×10^6", *Journal of Fluid Mechanics 109*, 239–251 (1981).